Hindawi Publishing Corporation
Mathematical Problems in Engineering
Volume 2013, Article ID 726721, 10 pages
http://dx.doi.org/10.1155/2013/726721

Research Article

Fractional Resonance-Based $RL_\beta C_\alpha$ Filters

Todd J. Freeborn,[1] Brent Maundy,[1] and Ahmed Elwakil[2]

[1] *Department of Electrical and Computer Engineering, University of Calgary, 2500 University Drive NW, Calgary, AB, Canada T2N 1N4*
[2] *Department of Electrical and Computer Engineering, University of Sharjah, P.O. Box 27272, Sharjah, UAE*

Correspondence should be addressed to Todd J. Freeborn; todd.freeborn@gmail.com

Received 17 September 2012; Accepted 20 December 2012

Academic Editor: József Kázmér Tar

We propose the use of a fractional order capacitor and fractional order inductor with orders $0 \leq \alpha, \beta \leq 1$, respectively, in a fractional $RL_\beta C_\alpha$ series circuit to realize fractional-step lowpass, highpass, bandpass, and bandreject filters. MATLAB simulations of lowpass and highpass responses having orders of $(\alpha + \beta) = 1.1$, 1.5, and 1.9 and bandpass and bandreject responses having orders of 1.5 and 1.9 are given as examples. PSPICE simulations of 1.1, 1.5, and 1.9 order lowpass and 1.0 and 1.4 order bandreject filters using approximated fractional order capacitors and fractional order inductors verify the implementations.

1. Introduction

Fractional calculus, the branch of mathematics concerning differentiations and integrations to noninteger order, has been steadily migrating from the theoretical realms of mathematicians into many applied and interdisciplinary branches of engineering [1]. These concepts have been imported into many broad fields of signal processing having many diverse applications, which include electromagnetics [2], wave propagation in human cancellous bone [3], state-of-charge estimation in batteries [4], thermal systems [5], and more. From the import of these concepts into electronics for analog signal processing has emerged the field of fractional order filters. This import into filter design has yielded much recent progress in theory [6–9], noise analysis [10], stability analysis [11], and implementation [12–14]. These filter circuits have all been designed using the fractional Laplacian operator, s^α, because the algebraic design of transfer functions are much simpler than solving the difficult time domain representations of fractional derivatives. A fractional derivative of order α is given by the Caputo derivative [15] as

$$ {}_a^C D_t^\alpha f(t) = \frac{1}{\Gamma(\alpha - n)} \int_a^t \frac{f^{(n)}(\tau)\, d\tau}{(t-\tau)^{\alpha+1-n}}, \tag{1} $$

where $\Gamma(\cdot)$ is the gamma function and $n - 1 \leq \alpha \leq n$. We use the Caputo definition of a fractional derivative over other approaches because the initial conditions for this definition take the same form as the more familiar integer-order differential equations. Applying the Laplace transform to the fractional derivative of (1) with lower terminal $a = 0$ yields

$$ \mathcal{L}\left\{ {}_0^C D_t^\alpha f(t) \right\} = s^\alpha F(s) - \sum_{k=0}^{n-1} s^{\alpha-k-1} f^{(k)}(0), \tag{2} $$

where s^α is also referred to as the fractional Laplacian operator. With zero initial conditions, (2) can be simplified to

$$ \mathcal{L}\left\{ {}_0^C D_t^\alpha f(t) \right\} = s^\alpha F(s). \tag{3} $$

Therefore it becomes possible to define a general fractance device with impedance proportional to s^α [16], where the traditional circuit elements are special cases of the general device when the order is −1, 0, and 1 for a capacitor, resistor, and inductor, respectively. The expressions of the voltage across a traditional capacitor and inductor are defined by integer order integration and differentiation, respectively, of the current through them. We can expand these devices to

the fractional domain using integrations and differentiations of non-integer order. Then the time domain expressions for the voltage across the fractional order capacitor and fractional order inductor become

$$v_C^{\alpha}(t) = \frac{1}{C\Gamma(\alpha)} \int_0^t \frac{i(\tau)}{(t-\tau)^{1-\alpha}} d\tau,$$
$$v_L^{\beta}(t) = L \frac{d^{\beta} i(t)}{dt^{\beta}}, \tag{4}$$

where $0 \leq \alpha, \beta \leq 1$ are the fractional orders of the capacitor and inductor, respectively, $i(t)$ is the current through the devices, C is the capacitance with units $\mathrm{F/s}^{1-\alpha}$, L is the inductance with units $\mathrm{H/s}^{1-\beta}$, and [s] is a unit of time not to be mistaken with the Laplacian operator. Note that we will refer to the units of these devices as [F] and [H] for simplicity.

By applying the Laplace transform to (4), with zero initial conditions, the impedances of these fractional order elements are given as $Z_C^{\alpha}(s) = 1/s^{\alpha}C$ and $Z_L^{\beta}(s) = s^{\beta}L$ for the fractional order capacitor and fractional order inductor, respectively. Using these fractional elements in circuits increases the range of responses that can be realized, expanding them from the narrow integer subset to the more general fractional domain. While these devices are not yet commercially available, recent research regarding their manufacture and production shows very promising results [17, 18]. Therefore, it is becoming increasingly important to develop the theory behind using these fractional elements so that when they are available their unique characteristics can be fully taken advantage of.

While a thorough stability analysis of the fractional $RL_{\beta}C_{\alpha}$ circuit has been presented in [11], the full range of filter responses possible with this topology have not. In this paper we examine the responses possible using a fractional order capacitor and fractional order inductor with orders of $0 \leq \alpha, \beta \leq 1$ in a series $RL_{\beta}C_{\alpha}$ circuit to realize fractional step filters. With this topology, fractional lowpass, highpass, bandpass, and bandreject filters of order $(\alpha + \beta)$ are realized. MATLAB simulations of lowpass and highpass responses having orders of $(\alpha + \beta) = 1.1$, 1.5, and 1.9 and bandpass and bandreject having orders of 1.5 and 1.9 are presented. PSPICE simulations of 1.1, 1.5, and 1.9 order lowpass and 1.0 and 1.4 order bandreject filters are presented using approximations of both fractional order capacitors and fractional order inductors to verify the $RL_{\beta}C_{\alpha}$ circuit and its implementation.

2. Fractional Responses

The traditional RLC circuit uses standard capacitors and inductors with which only 2nd order filter responses can be realized. We can further generalize this filter to the fractional domain by introducing fractional orders for both frequency-dependent elements. This approach of replacing traditional components with fractional components has previously been investigated for fractional order capacitors in the Sallen-Key filter, Kerwin-Huelsman-Newcomb biquad [7], and Tow-Thomas biquad [14]. The addition of the two fractional parameters allows the $RL_{\beta}C_{\alpha}$ circuit to realize any order $0 \leq \alpha + \beta \leq 2$. With this modification fractional lowpass, highpass, bandpass, and bandreject filter responses requiring only rearrangement of the series components are realizable. The topologies to realize these four fractional order filter responses are shown in Figure 1.

2.1. Fractional Lowpass Filter (FLPF). The circuit shown in Figure 1(a) can be used to realize a lowpass filter response with a transfer function given by

$$T_{\mathrm{FLPF}}(s) = \frac{V_o(s)}{V_{\mathrm{in}}(s)} = \frac{1/LC}{s^{\alpha+\beta} + s^{\alpha}(R/L) + 1/LC}. \tag{5}$$

This transfer function realizes an FLPF response with DC gain of 1, high frequency gain of zero, and fractional attenuation of $-20(\alpha + \beta)$ dB/decade in the stopband. With the magnitude of (5) given as

$$\begin{aligned} &\left|T_{\mathrm{FLPF}}(\omega)\right| \\ &\quad = \Big(2RLC^2\omega^{2\alpha+\beta}\cos(0.5\pi\beta) + 2RC\omega^{\alpha}\cos(0.5\alpha\pi) \\ &\qquad + 2LC\omega^{\beta+\alpha}\cos\left(0.5(\beta+\alpha)\pi\right) \\ &\qquad + R^2C^2\omega^{2\alpha} + L^2C^2\omega^{2\beta+2\alpha} + 1\Big)^{-1/2}. \end{aligned} \tag{6}$$

The MATLAB simulated magnitude responses of (5) with fractional orders of $\alpha + \beta = 1.1$, 1.5, and 1.9 with $\beta = 1$, $R = 1\,\Omega$, $L = 1\,\mathrm{H}$, and $C = 1\,\mathrm{F}$ are illustrated in Figure 2, respectively. From the magnitude responses of Figure 2 we see stopband attenuations and $\omega_{3_{\mathrm{dB}}}$ frequencies of -22, -30, and -38 dB/decade and 1.623×10^{-4}, 0.3995, and 1.209 rad/s for the 1.1, 1.5, and 1.9 order FLPFs, respectively. This confirms the decreasing fractional step of the stopband attenuation as the order, $(\alpha + \beta)$, increases.

The half power frequency, $\omega_{3_{\mathrm{dB}}}$, can be found by numerically solving the following equation:

$$\left|T_{\mathrm{FLPF}}\left(\omega_{3_{\mathrm{dB}}}\right)\right| = \frac{1}{\sqrt{2}} \tag{7}$$

for $\omega_{3_{\mathrm{dB}}}$. Solving (7) for fixed values of β when α is varied from 0.1 to 1 in steps of 0.01 and $R = L = C = 1$ yields the values given in Figure 3. These values show a general trend that as both α and β increase, the half power frequency increases. It should be noted that all subsequent MATLAB simulations are performed for fixed values of β when α is varied in steps of 0.01 from 0.1 to 1.0 with all components fixed with values of $R = 1\,\Omega$, $L = 1\,\mathrm{H}$, and $C = 1\,\mathrm{F}$.

2.2. Fractional Highpass Filter (FHPF). The circuit shown in Figure 1(b) can be used to realize a highpass filter response with a transfer function given by

$$T_{\mathrm{FHPF}}(s) = \frac{V_o(s)}{V_{\mathrm{in}}(s)} = \frac{s^{\alpha+\beta}}{s^{\alpha+\beta} + s^{\alpha}(R/L) + 1/LC} \tag{8}$$

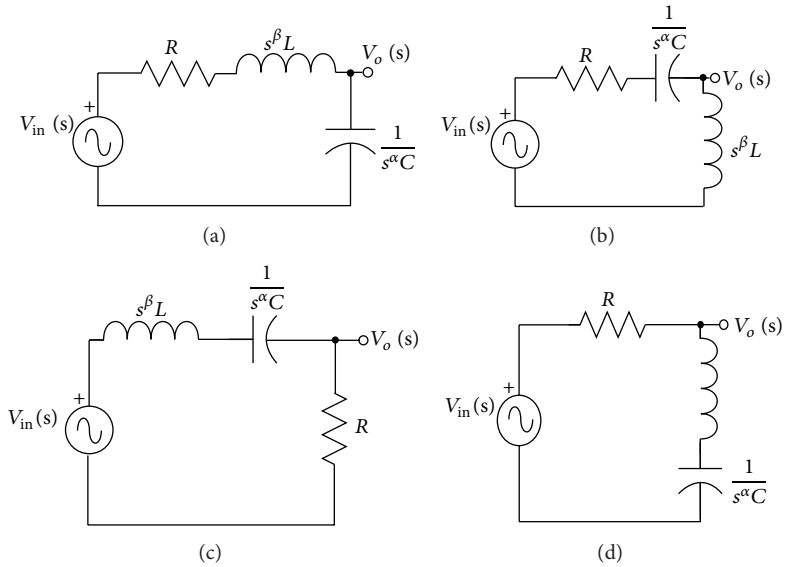

FIGURE 1: Fractional $RL_\beta C_\alpha$ topologies to realize $(\alpha + \beta)$ order (a) FLPF, (b) FHPF, (c) FBPF, and (d) FBRF responses.

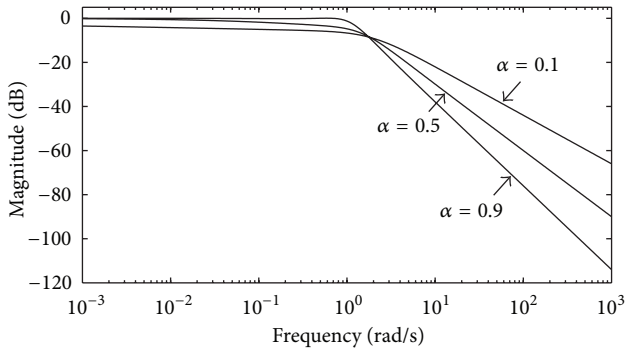

FIGURE 2: Simulated magnitude response of (5) when $\beta = 1, \alpha = 0.1$, 0.5, and 0.9 for $R = 1\,\Omega$, $L = 1$ H, and $C = 1$ F.

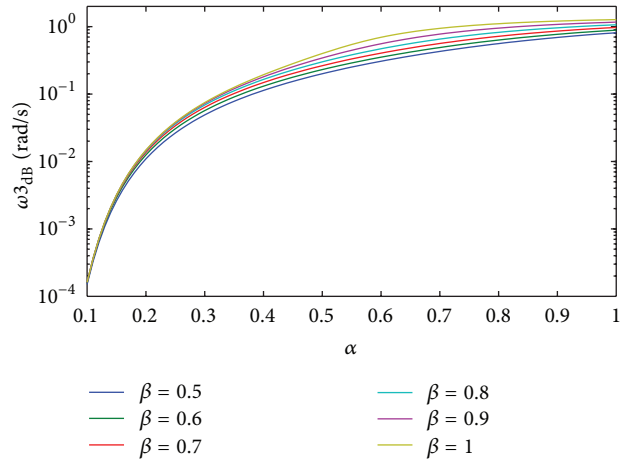

FIGURE 3: Half power frequencies of (5) for fixed values of β when α is varied from 0.1 to 1 in steps of 0.01 and $R = 1\,\Omega$, $L = 1$ H, and $C = 1$ F.

with DC gain of zero, high frequency gain of 1, and fractional attenuation of $20(\alpha + \beta)$ dB/decade in the stopband. The magnitude of (8) is given as

$$\begin{aligned}&\left|T_{\text{FHPF}}(\omega)\right| \\ &\quad = LC\omega^{\beta+\alpha}\left(2RLC^2\omega^{2\alpha+\beta}\cos\left(0.5\pi\beta\right)\right. \\ &\qquad + 2CR\omega^{\alpha}\cos\left(0.5\alpha\pi\right) \\ &\qquad + 2LC\omega^{\beta+\alpha}\cos\left(0.5\left(\beta+\alpha\right)\pi\right) \\ &\qquad \left.+R^2C^2\omega^{2\alpha} + L^2C^2\omega^{2\beta+2\alpha} + 1\right)^{-1/2}.\end{aligned} \tag{9}$$

The MATLAB simulated magnitude response of (8) with fractional orders of $\alpha + \beta = 1.1$, 1.5, and 1.9 when $R = 1\,\Omega$, $L = 1$ H, and $C = 1$ F are illustrated in Figure 4. From the magnitude responses of Figure 4 we see stopband attenuations and $\omega_{3_{\text{dB}}}$ frequencies of of 22, 30, and 38 dB/decade and 1.795, 1.232, and 0.8570 rad/s for the 1.1, 1.5, and 1.9 order FHPFs, respectively.

The half power frequency, $\omega_{3_{\text{dB}}}$, can be found by numerically solving the equation $|T_{\text{FHPF}}(\omega_{3_{\text{dB}}})| = 1/\sqrt{2}$ for $\omega_{3_{\text{dB}}}$. The values calculated with fixed β and varied α are shown in Figure 5. These values show a general trend that as both α and β increase, the half power frequency decreases.

2.3. Fractional Bandpass Filter (FBPF). The circuit shown in Figure 1(c) can be used to realize a bandpass filter response with a transfer function given by

$$T_{\text{FBPF}}(s) = \frac{V_o(s)}{V_{\text{in}}(s)} = \frac{s^\alpha (R/L)}{s^{\alpha+\beta} + s^\alpha (R/L) + 1/LC}. \tag{10}$$

This transfer function realizes an asymmetric FBPF response with DC and high frequency gains of zero and fractional

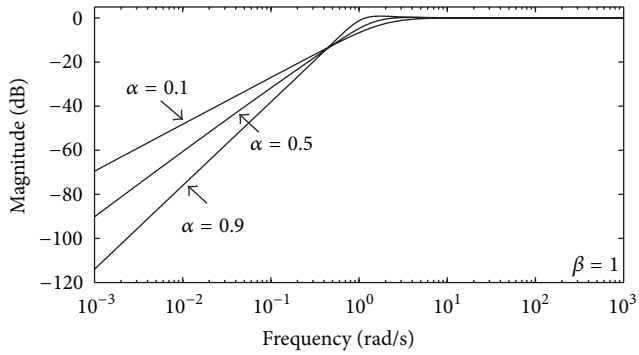

Figure 4: Simulated magnitude response of (8) when $\beta = 1, \alpha = 0.1$, 0.5, and 0.9 for $R = 1\,\Omega$, $L = 1$ H, and $C = 1$ F.

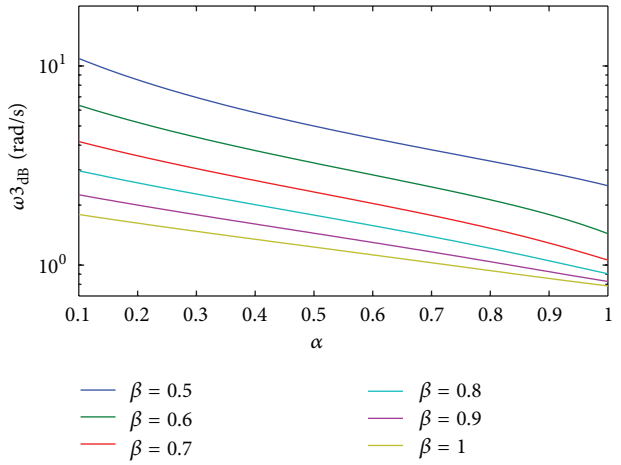

Figure 5: Half power frequencies of (8) for fixed values of β when α is varied from 0.1 to 1 in steps of 0.01 and $R = 1\,\Omega$, $L = 1$ H, and $C = 1$ F.

attenuations of 20α and -20β dB/decade for frequencies lower and higher, respectively, than the maxima frequency (ω_M). With the magnitude of (10) given as

$$\begin{aligned}\left|T_{\text{FBPF}}(\omega)\right| &= RC\omega^{\alpha}\left(2RLC^2\omega^{2\alpha+\beta}\cos(0.5\pi\beta)\right.\\ &\quad + 2RC\omega^{\alpha}\cos(0.5\alpha\pi)\\ &\quad + 2LC\omega^{\beta+\alpha}\cos\left(0.5(\beta+\alpha)\pi\right)\\ &\quad \left.+R^2\omega^{2\alpha}C^2 + L^2C^2\omega^{2\beta+2\alpha} + 1\right)^{-1/2}.\end{aligned} \tag{11}$$

The MATLAB simulated magnitude response of (10) with fractional orders of $\alpha + \beta = 1.5$, and 1.9 when $\beta = 1$, $R = 1\,\Omega$, $L = 1$ H, and $C = 1$ F are illustrated in Figure 6. From the simulated magnitude responses, we see that the low frequency stopband has attenuations of 10 and 18 dB/decade while the high frequency stopband maintains an attenuation of −20 dB/decade. The stopband attenuations closely match those predicted and confirm that the low and high frequency stopband attenuations are independent of each other (which is unique for fractional-order bandpass filters), with low frequency stopband attenuations dependent only on the order of the fractional capacitor, α, and the high frequency stopband only on the order of the fractional inductor, β.

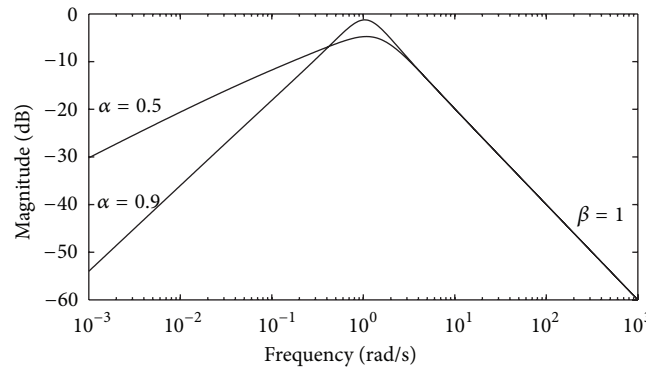

Figure 6: Simulated magnitude response of (10) when $\beta = 1$, $\alpha = 0.5$ and 0.9 for $R = 1\,\Omega$, $L = 1$ H, and $C = 1$ F.

Table 1: Maxima frequency and corresponding magnitude, half power frequencies, and quality factors of FBPFs given in Figure 6.

α	ω_M (rad/s)	$\lvert T(\omega_M)\rvert$ (dB)	ω_1, ω_2 (rad/s)	Q
0.5	1.082	−4.747	0.3173, 2.4171	0.5151
0.9	1.038	−1.246	0.5773, 1.7961	0.8516

Table 2: Minima frequency and corresponding magnitude, half power frequencies, and quality factors of FBRFs given in Figure 10.

α	ω_m (rad/s)	$\lvert T(\omega_m)\rvert$ (dB)	ω_1, ω_2 (rad/s)	Q
0.5	0.8974	−7.241	0.2145, 1.850	0.5486
0.9	0.9989	−17.35	0.5309, 1.701	0.8539

The maxima frequency can be found by numerically solving the following equation:

$$\frac{d\left|T_{\text{FBPF}}(\omega)\right|}{d\omega} = 0 \tag{12}$$

for ω. Solving (12) for varying α and fixed values of β yields the maxima frequencies given in Figure 7(a). The quality factor, Q, can be found by numerically solving

$$\left|T_{\text{FBPF}}(\omega)\right| = \frac{\left|T_{\text{FBPF}}(\omega_M)\right|}{\sqrt{2}} \tag{13}$$

for its two real roots, ω_1 and ω_2, and then evaluating $Q = \omega_M/|\omega_1 - \omega_2|$. Solving these equations numerically for varying α and fixed values of β yields the quality factors given in Figure 7(b). While there is no clear trend for ω_M, Q shows an increase with increasing order for fixed β when $R = 1\,\Omega$, $L = 1$ H, and $C = 1$ F. The maxima frequency (ω_M), maximum magnitude ($|T(\omega_M)|$), half power frequencies, ($\omega_{1,2}$), and quality factors (Q) of the FBPF responses shown in Figure 6, solved numerically as described previously, are given in Table 1.

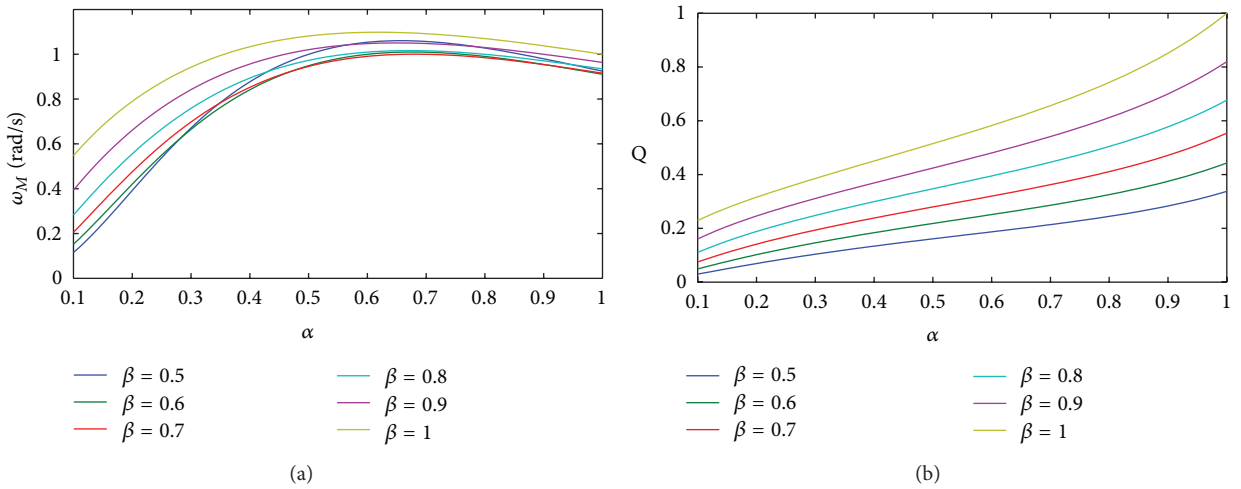

FIGURE 7: (a) Maxima frequencies and (b) quality factors of (10) for fixed values of β when α is varied from 0.1 to 1 in steps of 0.01 and $R = 1\,\Omega$, $L = 1\,\text{H}$, $C = 1\,\text{F}$.

It is possible to increase the quality factor of these circuits by decreasing the value of R for fixed order and values of L and C. The quality factors of the FBPF when $\beta = 1$, $L = 1\,\text{H}$, and $C = 1\,\text{F}$ for α and R varied from 0.1 to 1 in steps of 0.01 are given in Figure 8. From this figure, we can see that the increasing Q is more pronounced with higher orders.

2.4. Fractional Bandreject Filter (FBRF). The circuit shown in Figure 1(d) is able to realize a bandreject filter response with a transfer function given by

$$T_{\text{FBRF}}(s) = \frac{V_o(s)}{V_{\text{in}}(s)} = \frac{s^{\alpha+\beta} + 1/LC}{s^{\alpha+\beta} + s^{\alpha}(R/L) + 1/LC}. \tag{14}$$

This transfer function realizes an asymmetric FBRF response with DC and high frequency gains of 1. With the magnitude of (14) given as

$$\begin{aligned}&\left|T_{\text{FBRF}}(\omega)\right| \\ &= \left(L^2C^2\omega^{2\beta+2\alpha} + 2LC\omega^{\beta+\alpha}\cos\left(0.5(\alpha+\beta)\pi\right) + 1\right)^{1/2} \\ &\quad / \left(2RC\omega^{\alpha}\cos(0.5\alpha\pi) + 2LC\omega^{\beta+\alpha}\cos\left(0.5(\alpha+\beta)\pi\right)\right. \\ &\quad \left. + C^2R^2\omega^{2\alpha} + 2RLC^2\omega^{2\alpha+\beta}\cos(0.5\pi\beta) + L^2C\omega^{2\beta+2\alpha} + 1\right)^{1/2}.\end{aligned} \tag{15}$$

The minima frequency, ω_m, can be found by numerically solving $d|T_{\text{FBRF}}(\omega)|/d\omega = 0$ for ω. Solving this equation when $R = 1\,\Omega$, $L = 1\,\text{H}$, and $C = 1\,\text{F}$ for fixed values of β when α is varied from 0.1 to 1 yields the values given in Figure 9(a), while Q, can be found by numerically solving $|T_{\text{FBRF}}(\omega)| = 1/\sqrt{2}$ for its two real roots, ω_1 and ω_2, and then evaluating $Q = \omega_m/|\omega_1 - \omega_2|$. The quality factor calculated for FBRFs while α is varied for fixed β is given in Figure 9(b), respectively, again, with the general trend showing that Q increases with increasing order.

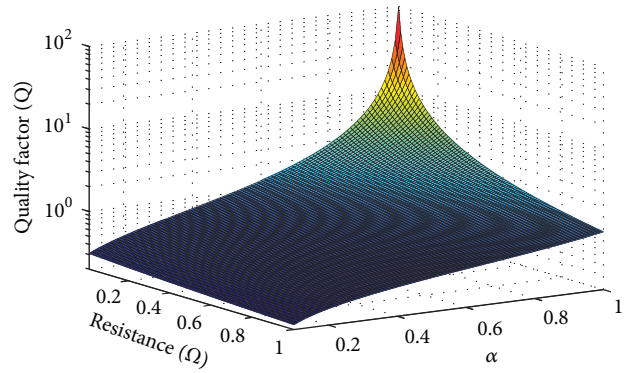

FIGURE 8: Quality factors of (10) for $\beta = 1$, $L = 1\,\text{H}$, $C = 1\,\text{F}$ when α and R are varied from 0.1 and 0.01, respectively, to 1 in steps of 0.01.

The MATLAB simulated magnitude responses of (14) with fractional orders of $\alpha + \beta = 1.5$ and 1.9 when $\beta = 1$, $R = 1\,\Omega$, $L = 1\,\text{H}$, and $C = 1\,\text{F}$ are illustrated in Figure 10. From this figure, we can clearly observe the asymmetric nature of this FBRF, with the attenuation of the low and high frequency stop bands dependent on the element orders of α and β, respectively. The minima frequency (ω_m), minimum magnitude ($|T(\omega_m)|$), half power frequencies ($\omega_{1,2}$), and quality factors (Q) of these responses are given in Table 2. It is possible to increase the quality factor of the FBRF by decreasing the value of R for fixed order and values of L and C. The quality factors of the FBRF when $\beta = 1$, $L = 1\,\text{H}$, and $C = 1\,\text{F}$ for α varied from 0.1 to 1 and R varied from 0.5 to 1 in steps of 0.01 are given in Figure 11. From this figure, we can see that like the FBPF the increasing Q is more pronounced with higher orders. It should be noted, though, that it is not possible to calculate a quality factor for FBRFs with both low order and resistance. The minima peak of these filters increases with decreasing order and resistance and when the minima increases above $1/\sqrt{(2)}$ it is not possible to calculate the quality factor using the previous definition.

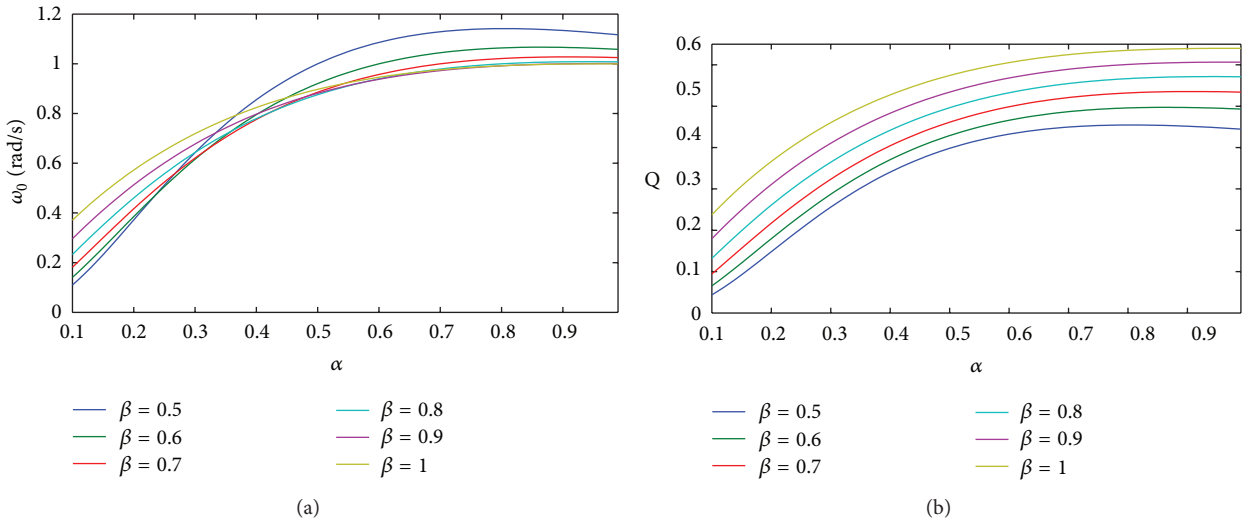

FIGURE 9: (a) Minima frequencies and (b) quality factors of FBRFs for fixed values of β when α is varied from 0.1 to 1 in steps of 0.01 and $R = 1\ \Omega$, $L = 1$ H, and $C = 1$ F.

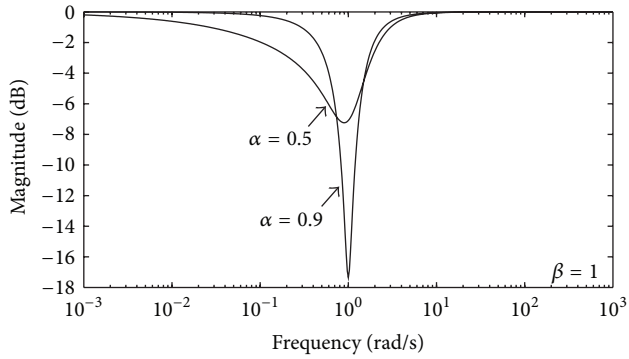

FIGURE 10: Simulated magnitude response of (14) when $\beta = 1$, $\alpha = 0.5$ and 0.9 for $R = 1\ \Omega$, $L = 1$ H, and $C = 1$ F.

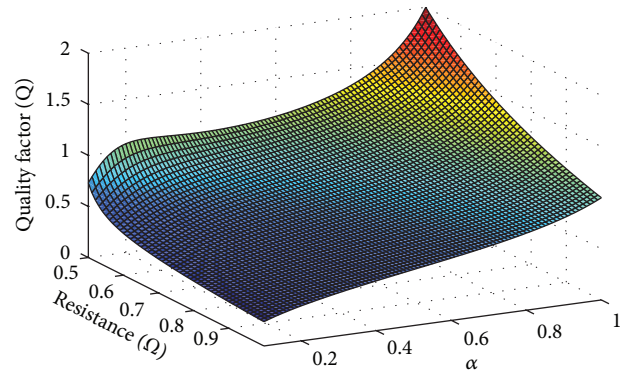

FIGURE 11: Quality factors of (14) for $\beta = 1$, $L = 1$ H, $C = 1$ F when α and R are varied from 0.1 and 0.5, respectively, to 1 in steps of 0.01.

3. Circuit Simulation Results

Although there is currently much progress regarding the realization of fractional order capacitors [17, 18], there are no commercial devices using these processes available to implement these circuits. As well, even though supercapacitors have been shown to exhibit fractional impedances [19, 20], their high capacitance and limited order ($0.5 \leq \alpha \leq 0.6$) limit their usefulness in signal processing circuits. Until commercial devices with the desired characteristics become available, integer order approximations must be used to realize fractional circuits. There are many methods to create an approximation of s^{α} that include continued fraction expansions (CFEs) as well as rational approximation methods [21]. These methods present a large array of approximations with the accuracy and approximated frequency band increasing as the order of the approximation increases. Here, a CFE method [22] was selected to model the fractional order capacitors for PSPICE simulations. Collecting eight terms of the CFE yields a 4th order approximation of the fractional capacitor that can be physically realized using the RC ladder network in Figure 12.

Now, while an RC ladder can be used to approximate a fractional order capacitor, this same topology cannot realize a fractional order inductor as it would require negative component values. However, we can use a fractional order capacitor as a component in a general impedance converter circuit (GIC), shown in Figure 13, which is used to simulate a grounded impedance [23]. Figure 13 realizes the impedance

$$Z = \frac{s^{\beta} C R_1 R_3 R_5}{R_2} \tag{16}$$

simulating a fractional inductor of order β with inductance $L = CR_1R_3R_5/R_2$.

Using both the approximated fractional order capacitor and fractional order inductor, we can realize the FBRF shown in Figure 1(d) with orders $\alpha + \beta = 1.0$ and $\alpha + \beta = 1.4$ when $\alpha = 0.5$. The realized circuit is given in Figure 14 with the RC ladder shown as the inset for the fractional order capacitor and the GIC circuit as the inset for the fractional order inductor. The R, L, and C values

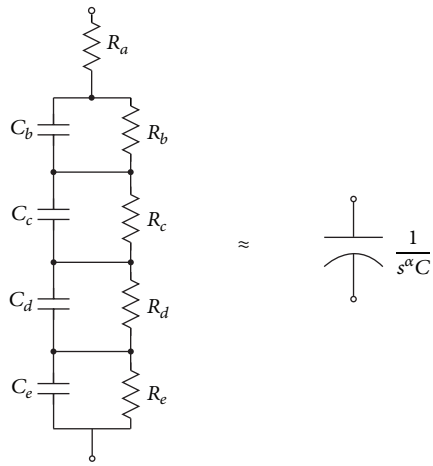

Figure 12: RC ladder structure to realize a 4th order integer approximation of a fractional order capacitor.

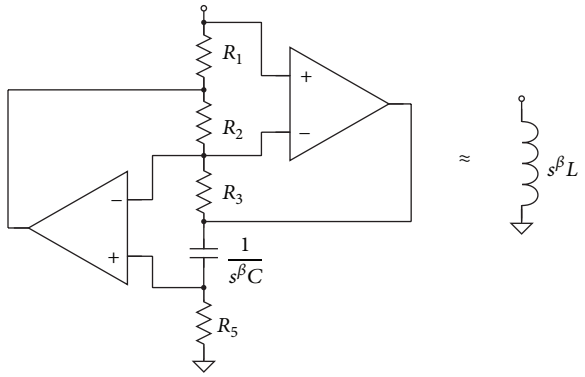

Figure 13: GIC topology to simulate a grounded fractional order inductor using a fractional order capacitor as a component.

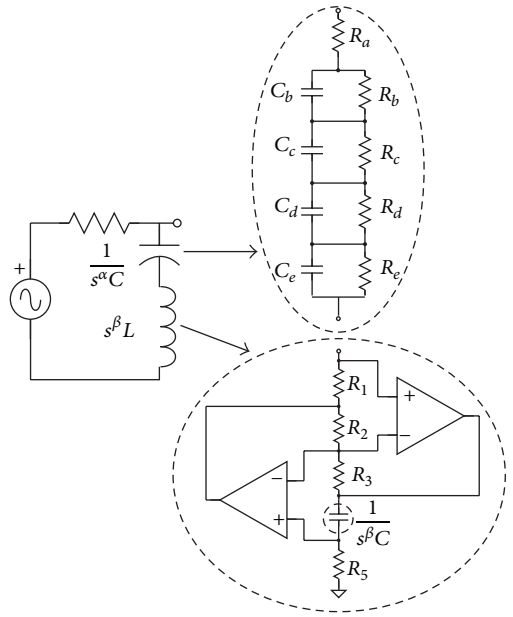

Figure 14: Approximated FBRF circuit realized with RC ladder approximation of fractional order capacitors and GIC approximation of a fractional order inductor.

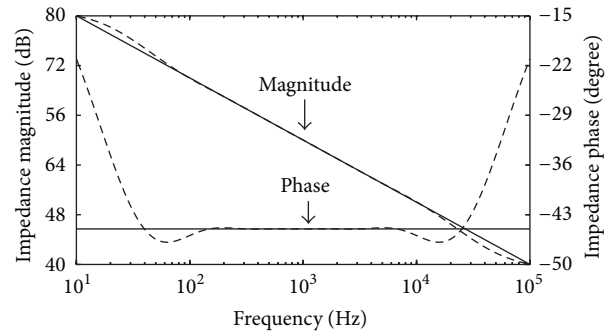

Figure 15: Magnitude and phase response of the approximated fractional order capacitor (dashed) compared to the ideal (solid) with capacitance of 12.6 μF and order 0.5 after scaling to a center frequency of 1 kHz.

Table 3: Component values to realize 1.0 and 1.4 order FBRFs for $\alpha = 0.5$ and $\beta = 0.5$ and 0.9, respectively, after magnitude scaled by a factor of 1000 and frequency shifted to 1 kHz.

Component	Values	
	$\beta = 0.5$	$\beta = 0.9$
R (Ω)	1000	1000
L (H)	12.6	0.382
C (μF)	12.6	12.6

required to realize these circuits after applying a magnitude scaling of 1000 and frequency scaling to 1 kHz are given in Table 3. The component values required for the 4th order approximation of the fractional capacitances with values of 12.6 and 0.382 μF and orders of 0.5 and 0.9, respectively, using the RC ladder network in Figure 12, shifted to a center frequency of 1 kHz, are given in Table 4. The magnitude and phase of the ideal (solid line) and 4th order approximated (dashed) fractional order capacitor with capacitance 12.6 μF and order $\alpha = 0.5$, shifted to a center frequency of 1 kHz, are presented in Figure 15. From this figure we observe that the approximation is very good over almost 4 decades, from 200 Hz to 70 kHz, for the magnitude and almost 2 decades, from 200 Hz to 6 kHz, for the phase. In these regions, the deviation of the approximation from ideal does not exceed 1.23 dB and 0.23° for the magnitude and phase, respectively. The simulated fractional order inductors of 12.6 and 0.382 H can be realized using fractional capacitances of 12.6 and 0.382 μF, respectively, when $R_1 = R_2 = R_3 = R_5 = 1000\,\Omega$.

Using the component values in Tables 3 and 4, the approximated FBRF, shown in Figure 14, was simulated in PSPICE using MC1458 op amps to realize responses of order $(\alpha + \beta) = 1.0$ and 1.4 when $\alpha = 0.5$ and $\beta = 0.5$ and 0.9. The PSPICE simulated magnitude responses (dashed lines) compared to the ideal responses (solid lines) are shown in Figure 16. We can clearly see from the magnitude response of both the MATLAB and PSPICE simulated responses that this filter does realize a fractional band reject response and that the simulation shows good agreement with the ideal response observing both symmetric and asymmetric characteristics for the 1.0 and 1.4 order filters, respectively. Note, though,

Table 4: Component values to realize 4th order approximations of fractional order capacitors with a center frequency of 1 kHz.

Component	Values				
	$C = 1\,\mu$F $\alpha = 0.1$	$C = 1\,\mu$F $\alpha = 0.5$	$C = 12.6\,\mu$F $\alpha = 0.5$	$C = 0.382\,\mu$F $\alpha = 0.9$	$C = 1\,\mu$F $\alpha = 0.9$
R_a (Ω)	274.7 k	1.402 k	111.1	6.8	2.6
R_b (Ω)	81.9 k	3.17 k	251.7	43.3	16.5
R_c (Ω)	56.1 k	4.78 k	378.7	130.7	49.9
R_d (Ω)	66.3 k	11.2 k	888.9	670.4	255.9
R_e (Ω)	154.1 k	92.9 k	7369.7	146189.7	55789.8
C_b (nF)	0.165	6.64	68.9	705	1846
C_c (μF)	0.0015	0.023	0.296	1.13	2.97
C_d (μF)	0.0052	0.043	0.537	1.03	2.69
C_e (μF)	0.015	0.055	0.695	0.207	0.544

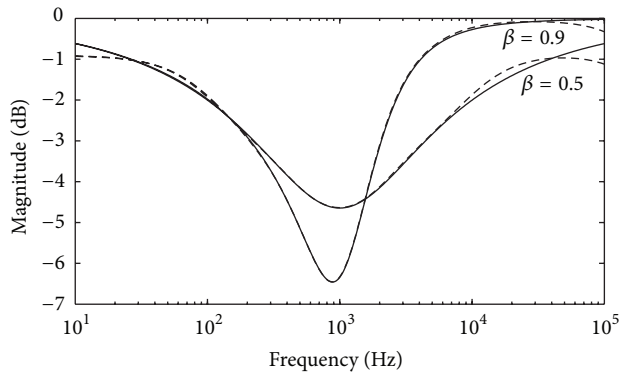

Figure 16: PSPICE simulations using Figure 14 compared to ideal simulations of (14) as dashed and solid lines, respectively, to realize approximated FBRFs of orders $\alpha + \beta = 1.0$ and 1.4 when $\alpha = 0.5$.

that the PSPICE simulations deviate from the MATLAB simulated transfer function at low and high frequencies, which is a result of using the 4th order approximation of the fractional order capacitors. We highlight that this filter presents two characteristics not possible using integer order filters: (a) bandreject responses have not been possible from integer order filters with order less than 2 and (b) asymmetric responses with independent control of stopband attenuation have never been presented.

3.1. Fractional Bruton Transformation. The Bruton transformation applies an impedance transformation to each element of a passive ladder circuit to create an active circuit realization using the concept of frequency-dependent negative resistance that does not require the use of inductors [24]. This method can be expanded to the fractional-order domain to remove the fractional order inductor from the $RL_\beta C_\alpha$ circuit. Where the integer order transformation scales each element by $1/s$, the fractional Bruton transformation scales each element by $1/s^\beta$. Applying this scaling to a resistor transforms it to a fractional order capacitor, a fractional order inductor to a resistor, and a fractional order capacitor to a new fractional element of order $0 \le \alpha + \beta \le 1$. This new fractional element can be a resistor, capacitor, or frequency-dependent negative resistor (FDNR) when $\alpha + \beta = 0$, 1, and 2, respectively. Note that we will use the units of [Ω] when referring to this fractional element in order to remain consistent with the FDNR, whose symbol we are also using to represent this element. The FLPF of Figure 1(a) after applying the fractional Bruton transformation is shown in Figure 17. The transfer function of this transformed circuit is given by

$$T_{\text{FLPF}}(s) = \frac{V_o(s)}{V_{\text{in}}(s)} = \frac{1/R_b D_b}{s^{\alpha+\beta} + s^\alpha/R_b C_b + 1/R_b D_b}, \qquad (17)$$

where $C_b = 1/R$, $R_b = L$, and $D_b = C$ for the transfer function to be equivalent to (5).

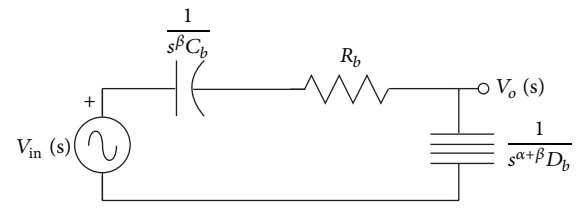

Figure 17: FLPF of Figure 1(a) after applying the fractional Bruton transformation.

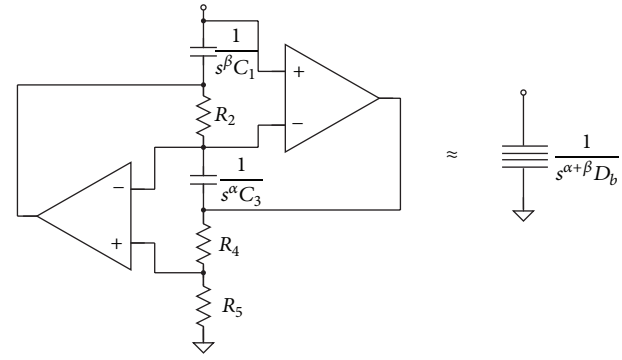

Figure 18: GIC topology to simulate a grounded fractional element of order $0 \le \alpha + \beta \le 2$ using two fractional order capacitors components.

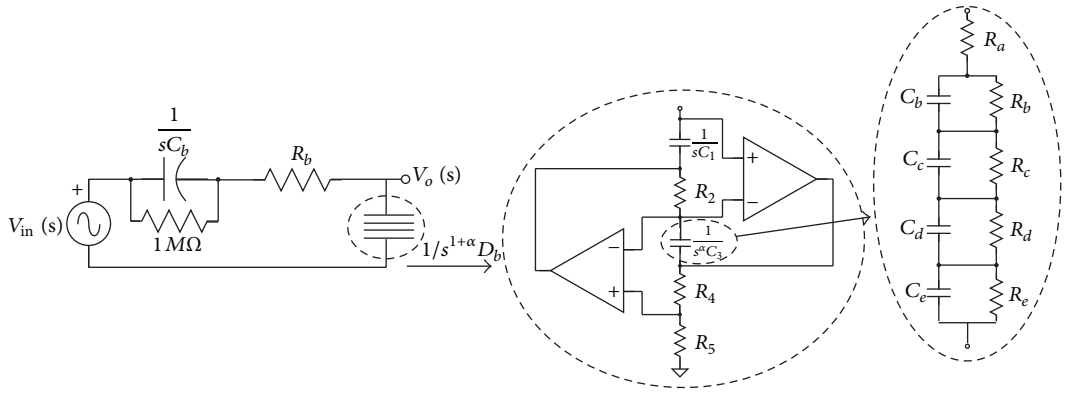

Figure 19: Approximated FLPF of Figure 17 realized with RC ladder approximations of fractional order capacitors and GIC approximation of a fractional element of order $(\alpha + \beta)$.

Table 5: Component values to realize fractional elements with GIC topology of Figure 18.

Component	Values		
	D_b = 66.38 nΩ Order = 1.1	D_b = 2.01 nΩ Order = 1.5	D_b = 60.74 pΩ Order = 1.9
C_1 (μF), β	1, 1	1, 1	1, 1
C_3 (μF), α	1, 0.1	1, 0.5	1, 0.9
R_2 (Ω)	66.38 k	2.01 k	60.74
R_4 (Ω)	1000	1000	1000
R_5 (Ω)	1000	1000	1000

This new fractional element can be realized using a GIC with two fractional order capacitors, this topology is shown in Figure 18 and has an impedance

$$Z_D = \frac{R_5}{s^{\alpha+\beta} C_1 C_3 R_2 R_4} \tag{18}$$

simulating a fractional element with impedance $D_b = C_1 C_3 R_2 R_4 / R_5$. A GIC has also previously been employed to realize a fractional order capacitor of 36 μF and $\alpha = 1.6$ in [7]. Using the topology of Figure 17 to simulate the FLPFs of Figure 2, magnitude scaled by 1000 and frequency shifted to 1 kHz, requires $C_b = 0.1592\,\mu$F, $R_b = 1000\,\Omega$, and D_b = (66.38 n, 2.01 n, 60.74 p)Ω for the $(\alpha + \beta) = 1.1$, 1.5, and 1.9 order filters, respectively, when $\beta = 1$. The components required to simulate the impedance of the fractional element using the GIC topology are given in Table 5, with the values of the fractional order capacitor C_3 approximated with the RC ladder of Figure 12 given in Table 4.

The approximated FLPF, shown in Figure 19, was simulated in PSPICE using MC1458 op amps to realize a $(\alpha + \beta) = 1.9$ order filter when $\beta = 1$. The PSPICE simulated magnitude responses (dashed lines) compared to the ideal responses (solid lines) are shown in Figure 20. Note that a 1 MΩ resistor has been added to bypass the capacitor and provide a DC path to the noninverting input terminal of the upper op amp in the fractional element realization for its bias current [23].

The PSPICE simulated magnitude responses of the FLPFs show very good agreement with the MATLAB simulated ideal response. Verifying the fractional Bruton transformed FLPFs as well as the GIC realizations of a fractional element of order $(\alpha + \beta)$ using approximated fractional order capacitors. The deviations above 20 kHz can be attributed to the approximations of the fractional order capacitors and nonidealities of the op amps used to realize the fractional order inductors.

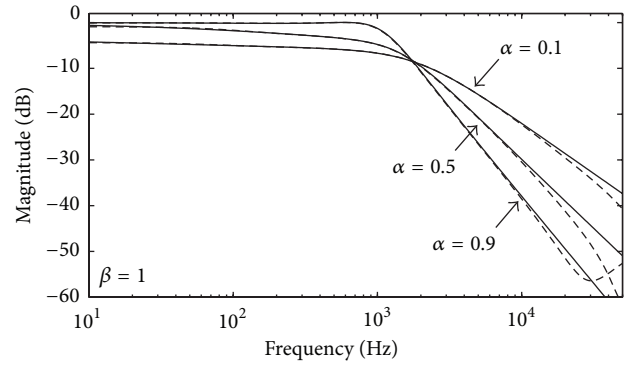

Figure 20: PSPICE simulation using Figure 19 compared to ideal simulations of (17) as dashed and solid lines, respectively, to realize approximated FLPF of order $\alpha + \beta = 1.9$ when $\beta = 1$.

4. Conclusion

We have proposed modifying the traditional series RLC circuit to use a fractional order capacitor and fractional order inductor to realize a fractional $RL_\beta C_\alpha$ circuit that is capable of realizing fractional lowpass, highpass, bandpass, and bandreject filter responses of order $0 < \alpha + \beta \leq 2$ requiring only modification of the element arrangement. This topology can realize bandpass or bandreject responses with order less than 2 which are not possible using an integer order circuit. In addition, these proposed bandpass and bandreject filters show asymmetric bandpass characteristics with independent control of the stopband attenuations through manipulation of the fractional elements orders, which is not easily accomplished using integer order filters. We have also shown how to realize a new fractional element of order $(\alpha +$

$\beta) \leq 2$ and a fractional order inductor using fractional order capacitors in a GIC circuit. PSPICE simulations of FBRFs and FLPFs verify the fractional characteristics of these circuits as well as the proposed realizations using approximated fractional elements.

Acknowledgments

T. J. Freeborn would like to acknowledge Canada's National Sciences and Engineering Research Council (NSERC), Alberta Innovates-Technology Futures, and Alberta Advanced Education and Technology for their financial support of this research through their graduate student scholarships.

References

[1] A. S. Elwakil, "Fractional-order circuits and systems: an emerging interdisciplinary research area," *IEEE Circuits and Systems Magazine*, vol. 10, no. 4, pp. 40–50, 2010.

[2] J. A. Tenreiro Machado, I. S. Jesus, A. Galhano, and J. Boaventura Cunha, "Fractional order electromagnetics," *Signal Processing*, vol. 86, no. 10, pp. 2637–2644, 2006.

[3] N. Sebaa, Z. E. A. Fellah, W. Lauriks, and C. Depollier, "Application of fractional calculus to ultrasonic wave propagation in human cancellous bone," *Signal Processing*, vol. 86, no. 10, pp. 2668–2677, 2006.

[4] J. Sabatier, M. Aoun, A. Oustaloup, G. Grégoire, F. Ragot, and P. Roy, "Fractional system identification for lead acid battery state of charge estimation," *Signal Processing*, vol. 86, no. 10, pp. 2645–2657, 2006.

[5] J. D. Gabano and T. Poinot, "Fractional modelling and identification of thermal systems," *Signal Processing*, vol. 91, no. 3, pp. 531–541, 2011.

[6] A. G. Radwan, A. S. Elwakil, and A. M. Soliman, "Fractional-order sinusoidal oscillators: design procedure and practical examples," *IEEE Transactions on Circuits and Systems*, vol. 55, no. 7, pp. 2051–2063, 2008.

[7] A. G. Radwan, A. S. Elwakil, and A. M. Soliman, "On the generalization of second-order filters to the fractional-order domain," *Journal of Circuits, Systems and Computers*, vol. 18, no. 2, pp. 361–386, 2009.

[8] A. Soltan, A. G. Radwan, and A. M. Soliman, "Butterworth passive filter in the fractional order," in *Proceedings of the International Conference on Microelectronics (ICM '11)*, pp. 1–5, Hammamet, Tunisia, 2011.

[9] P. Ahmadi, B. Maundy, A. S. Elwakil, and L. Belostostski, "High-quality factor asymmetric-slope band-pass filters: a fractional-order capacitor approach," *IET Circuits, Devices & Systems*, vol. 6, no. 3, pp. 187–197, 2012.

[10] A. Lahiri and T. K. Rawat, "Noise analysis of single stage fractional-order low pass filter using stochastic and fractional calculus," *ECTI Transactions on Electronics and Communications*, vol. 7, no. 2, pp. 136–143, 2009.

[11] A. Radwan, "Stability analysis of the fractional-order $RL_{\beta}C_{\alpha}$ circuit," *Journal of Fractional Calculus and Applications*, vol. 3, no. 1, pp. 1–15, 2012.

[12] T. J. Freeborn, B. Maundy, and A. S. Elwakil, "Field programmable analogue array implementations of fractional step filters," *IET Circuits, Devices & Systems*, vol. 4, no. 6, pp. 514–524, 2010.

[13] B. Maundy, A. S. Elwakil, and T. J. Freeborn, "On the practical realization of higher-order filters with fractional stepping," *Signal Processing*, vol. 91, no. 3, pp. 484–491, 2011.

[14] T. J. Freeborn, B. Maundy, and A. S. Elwakil, "Fractional-step Tow-Thomas biquad filters," *Nonlinear Theory and Its Applications, IEICE (NOLTA)*, vol. 3, no. 3, pp. 357–374, 2012.

[15] I. Podlubny, *Fractional Differential Equations: An Introduction to Fractional Derivatives, Fractional Differential Equations, to Methods of Their Solution and some of Their Applications*, vol. 198, Academic Press, San Diego, Calif, USA, 1999.

[16] M. Nakagawa and K. Sorimachi, "Basic characteristics of a fractance device," *IEICE—Transactions on Fundamentals of Electronics, Communications and Computer Sciences E*, vol. 75, pp. 1814–1819, 1992.

[17] M. Sivarama Krishna, S. Das, K. Biswas, and B. Goswami, "Fabrication of a fractional order capacitor with desired specifications: a study on process identification and characterization," *IEEE Transactions on Electron Devices*, vol. 58, no. 11, pp. 4067–4073, 2011.

[18] T. Haba, G. Ablart, T. Camps, and F. Olivie, "Influence of the electrical parameters on the input impedance of a fractal structure realised on silicon," *Chaos, Solitons Fractals*, vol. 24, no. 2, pp. 479–490, 2005.

[19] J. J. Quintana, A. Ramos, and I. Nuez, "Identification of the fractional impedance of ultracapacitors," in *Proceedings of the 2nd Workshop on Fractional Differentiation and Its Applications (IFAC '06)*, pp. 289–293, 2006.

[20] A. Dzieliński, G. Sarwas, and D. Sierociuk, "Comparison and validation of integer and fractional order ultracapacitor models," *Advances in Difference Equations*, vol. 2011, article 11, 2011.

[21] I. Podlubny, I. Petráš, B. M. Vinagre, P. O'Leary, and Ľ. Dorčák, "Analogue realizations of fractional-order controllers," *Nonlinear Dynamics: An International Journal of Nonlinear Dynamics and Chaos in Engineering Systems*, vol. 29, no. 1–4, pp. 281–296, 2002.

[22] B. Krishna and K. Reddy, "Active and passive realization of fractance device of order 1/2," *Active and Passive Electronic Components*, vol. 2008, Article ID 369421, 5 pages, 2008.

[23] R. Schaumann and M. E. Van Valkenburg, *Design of Analog Filters*, Oxford University Press, 2001.

[24] L. T. Bruton, "Network transfer functions using the concept of frequency-dependent negative resistance," *IEEE Transactions on Circuit Theory*, vol. CT-16, no. 3, pp. 406–408, 1969.